PET and RFA: Avril reviews current approaches to characterizing masses and assessing treatment response after radiofrequency ablation and previews an article in this issue on the use of ^{18}F-FDG PET in this application. . . . . ***Page 1235***

Optimal α-emitters: Zalutsky summarizes challenges in identifying appropriate radionuclides for targeted α-particle therapy and highlights articles in this issue on the potential of α-labeled monoclonal antibodies in cancer treatment. . . ***Page 1238***

Pathologic response prediction: Cascini and colleagues assess the predictive value of changes in tumor ^{18}F-FDG uptake on PET during and after preoperative radiochemotherapy in patients with locally advanced rectal cancer. . . . . ***Page 1241***

Pinpointing prostate disease: Reske and colleagues evaluate the ability of ^{11}C-choline PET/CT to identify prostate carcinoma and to differentiate cancer tissue from normal prostate, benign prostate hyperplasia, and focal chronic prostatitis. . . . . ***Page 1249***

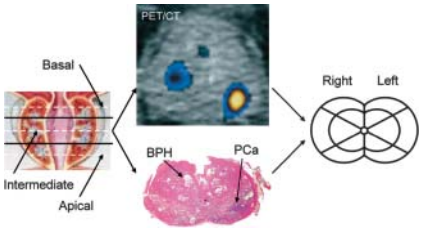

Significant information added: Yuan and colleagues compare ^{18}F-FDG PET/CT with side-by-side PET and CT images in the diagnosis of locoregional lymph node metastases in patients with esophageal squamous cell cancer. . . . . ***Page 1255***

Recommended as routine: Pryma and colleagues study the value of ^{18}F-FDG PET as part of initial postoperative staging and subsequent monitoring in patients with Hürthle cell thyroid cancer. . . ***Page 1260***

Characterizing disease progression: Bruzzi and colleagues evaluate the utility of PET/CT for detection of Richter's transformation of chronic lymphocytic leukemia into diffuse large cell lymphoma and assess the significance of these findings for prompt diagnosis and optimal management. . . . . ***Page 1267***

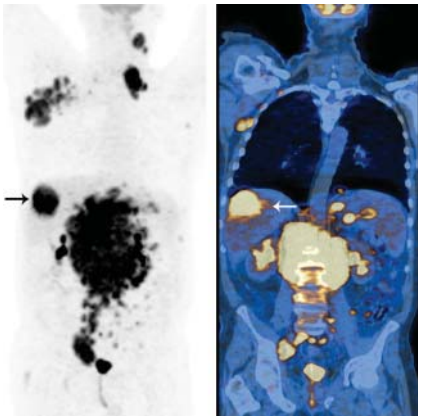

Spine imaging with PET: Rosen and colleagues report on the prevalence of abnormal spinal ^{18}F-FDG uptake and the relationship between findings on PET and the severity of degenerative spinal disease on CT. . . . . ***Page 1274***

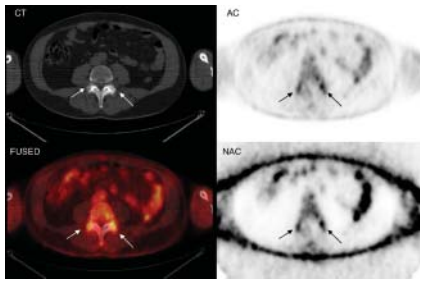

Targeting lung fibrosis: Lebtahi and colleagues investigate the expression of somatostatin receptors in the lungs of patients with idiopathic pulmonary fibrosis and correlate ^{111}In-octreotide uptake on SPECT with conventional functional and radiologic assessments of the condition. . . ***Page 1281***

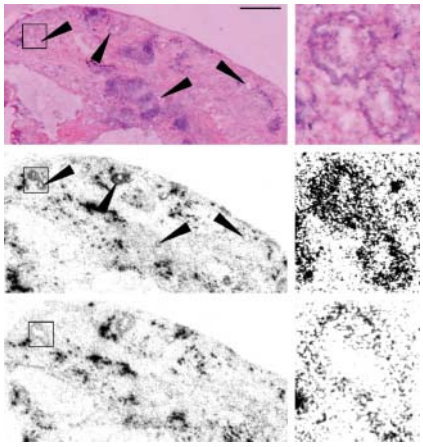

SPECT vs. CT in LV metrics: Schepis and colleagues compare the relative capabilities of ^{99m}Tc-gated SPECT and ECG-gated 64-slice CT in the assessment of left ventricular dimensions, muscle mass, and function in patients being evaluated for coronary artery disease. . . . . ***Page 1288***

Intracardiac stem cell therapy: Kang and colleagues employ PET to investigate the targeting capabilities and tissue distribution of intracoronary-injected peripheral hematopoietic stem cells labeled with ^{18}F-FDG in patients with myocardial infarction. . . . . ***Page 1295***

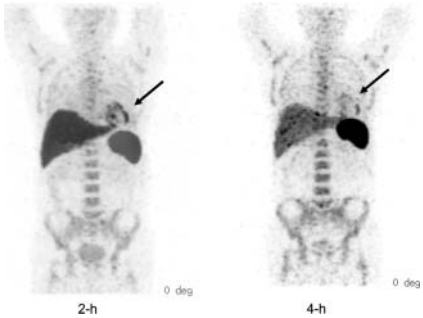

Obesity cardiac risk quantified: Elhendy and colleagues report on the accuracy of routine stress ^{99m}Tc-tetrofosmin myocardial perfusion imaging in predicting cardiac risk and overall mortality in patients who are obese. . . . . ***Page 1302***

Identifying myocardial viability: Slart and colleagues use both ^{18}F-FDG and ^{13}N-ammonia PET to evaluate the effects of nitrate administration on blood flow to chronically dysfunctional but viable myocardium in patients with chronic ischemic left ventricular dysfunction. . ***Page 1307***

More than attenuation correction: Goetze and colleagues review the frequency and significance of abnormal findings on the "nondiagnostic" CT portion of cardiac SPECT/CT scans in 200 patients. . . . . ***Page 1312***

Predicting antidepressive therapy response: Joe and colleagues use ^{99m}Tc-HMPAO SPECT to investigate progressive regional cerebral blood flow differences in patients who do and do not respond to citalopram therapy for major depression. . . . . ***Page 1319***

PET in lymphoma: Jhanwar and Straus provide a comprehensive review of the role of ^{18}F-FDG in the management of patients with lymphoma and discuss the potential for other PET tracers in accurately staging disease and predicting response to therapy. . . . . ***Page 1326***

Targeted therapy in leukemia: Glatting and colleagues evaluate the suitability of a ^{90}Y-labeled anti-CD45 monoclonal antibody for selectively delivering radiation to hematopoietic tissues in patients with refractory or relapsing acute myelogenous leukemia. . . . . ***Page 1335***

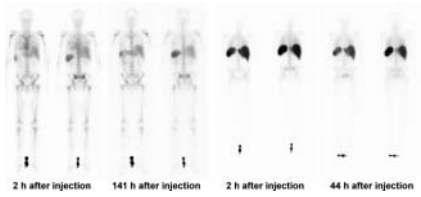

Enhanced effects of α-emitters: Elgqvist and colleagues investigate the efficacy of radioimmunotherapy using ^{211}At-labeled compounds in advanced ovarian cancer in a mouse model. . . . . ***Page 1342***

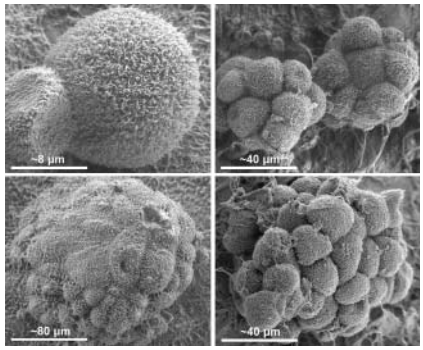

Assessing RFA response: Okuma and colleagues characterize normal lung tissue after radiofrequency ablation in a rabbit model and report on the suitability of dedicated small-animal PET for monitoring early therapeutic effects of ablation on lung tumors. . . . . ***Page 1351***

Novel PET tracer: Madar and colleagues explore in a canine model the kinetics and myocardial and whole-body biodistribution of an ^{18}F-labeled lipophilic cation for PET imaging. . . . . ***Page 1359***

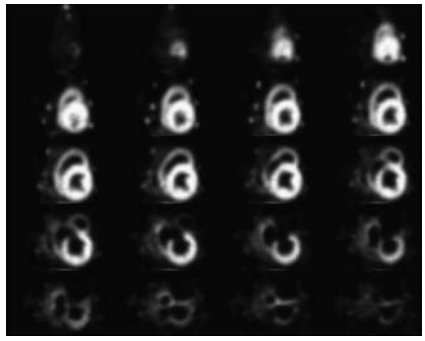

Imaging cardiac damage: Zhao and colleagues report on the development of a novel radiotracer designed to image apoptosis and necrosis in a rat model of reperfused acute myocardial infarction. . . . . ***Page 1367***

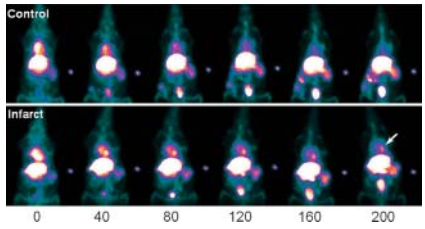

Thyroid treatment monitoring: Lubberink and colleagues determine the influence of large amounts of ^{131}I on PET image quality in the serial ^{124}I assessment of radiation dosimetry in therapy for thyroid cancer. . . . . ***Page 1375***

Cross-talk in thyroidal uptake: Bläser and colleagues conduct in vitro investigations on the mechanisms of signal transduction in ^{18}F-FDG and radioiodide uptake in an experimental thyroid cell line. . . ***Page 1382***

ON THE COVER

Precise and reliable assessment of left ventricular function and dimensions is prognostically important in cardiac patients. Comparison of SPECT and multislice CT for such assessments is pertinent because of the availability of hybrid scanners combining the 2 techniques. SPECT and multislice CT have been found to agree well over a wide range of clinically relevant values for left ventricular ejection fraction and functional parameters, but interchangeable use of the 2 techniques should be avoided for left ventricular volume, muscle mass, and regional wall motion.

SEE PAGE 1290